Polarization independence of extraordinary transmission trough 1D metallic gratings

T. Ongarello,[1,2,*] and F. Romanato,[1,2,3] P. Zilio,[1,2] M. Massari[1,2]

[1]*LaNN Laboratory for Nanofabrication of Nanodevices, Corso Stati Uniti 4, Padova, Italy*
[2]*University of Padova, Department of Physics, Via Marzolo 8, Padova, Italy*
[3]*IOM-TASC Natl. Lab. CNR-INFM, Basovizza S.S. 14 Km 163.5 Trieste, Italy*
**tommaso.ongarello@venetonanotech.it*

Abstract: Extraordinary optical transmission of 1D metallic gratings is studied. Experimental samples are fabricated by means of Electron Beam Lithography. The optical characterization is focused on far field transmission properties and in particular on polarization dependence of the incident light. A peculiar symmetry in transmission spectra at different polarization angles is shown; this symmetry is studied both experimentally, and numerically with FEM method. A comparison between numerical and experimental data is provided.

OCIS codes: (050.6624) Subwavelength structures; (250.5403) Plasmonics; (000.4930) Other topics of general interest.

References and links

1. T. W. Ebbesen, H. J. Lezec, H. F. Ghaemi, T. Thio, and P. A. Wolff, "Extraordinary optical transmission through sub-wavelength hole arrays," Nature **391**(6668), 667–669 (1998).
2. Y. Pang, C. Genet, and T. W. Ebbesen, "Optical transmission through sub-wavelength slit apertures in metallic films," Opt. Commun. **280**(1), 10–15 (2007).
3. A. Degiron, and T. W. Ebbesen, "The role of localized surface plasmon modes in the enhanced transmission of periodic sub-wavelength apertures," J. Opt. A, Pure Appl. Opt. **7**(2), S90–S96 (2005).
4. P. Lalanne, J. P. Hugonin, and J. C. Rodier, "Theory of surface plasmon generation at nanoslit apertures," Phys. Rev. Lett. **95**(26), 263902 (2005).
5. L. Salomon, F. Grillot, A. V. Zayats, and F. De Fornel, "Near-field distribution of optical transmission of periodic subwavelength holes in a metal film," Phys. Rev. Lett. **86**(6), 1110–1113 (2001).
6. J. A. Porto, F. J. Garcia-Vidal, and J. B. Pendry, "Transmission resonances on metallic gratings with very narrow slits," Phys. Rev. Lett. **83**(14), 2845–2848 (1999).
7. S. G. Rodrigo, F. J. Garcia-Vidal, and L. Martin-Moreno, "Influence on material properties on extraordinary optical transmission through hole arrays," Phys. Rev. B **77**(7), 075401 (2008).
8. F. J. Garcia-Vidal, L. Martin-Moreno, T. W. Ebbesen, and L. Kuipers, "Light passing trough subwavelength apertures," Rev. Mod. Phys. **82**(1), 729–787 (2010).
9. D. Crouse, and P. Keshavareddy, "Polarization independent enhanced optical transmission in one-dimensional gratings and device applications," Opt. Express **15**(4), 1415– 1427 (2007).
10. Y. Lu, M. H. Cho, Y. Lee, and J. Y. Rhee, "Polarization-independent extraordinary optical transmission in one-dimensional metallic gratings with broad slits," Appl. Phys. Lett. **93**(6), 061102 (2008).
11. F. Marquier, C. Arnold, M. Laroche, J. J. Greffet, and Y. Chen, "Degree of polarization of thermal light emitted by gratings supporting surface waves," Opt. Express **16**(8), 5305–5313 (2008).
12. A. Barbara, P. Quémerais, E. Bustarett, and T. Lopez-Rios, "Optical transmission through subwavelength metallic gratings," Phys. Rev. B **66**(16), 161403 (2002).
13. Y. Pang, C. Genet, and T. W. Ebbesen, "Optical transmission through subwavelength slit apertures in metallic films," Opt. Commun. **280**(1), 10–15 (2007).
14. D. Crouse, A. P. Hibbins, and M. J. Lockyear, "Tuning the polarization state of enhanced transmission in gratings," Appl. Phys. Lett. **92**(19), 191105 (2008).
15. S. Collin, G. Vincent, R. Haidar, N. Bardou, S. Rommeluère, and J. L. Pelouard, "Nearly perfect Fano transmission resonances through nanoslits drilled in a metallic membrane," Phys. Rev. Lett. **104**(2), 027401 (2010).
16. P. Zilio, D. Sammito, G. Zacco, and F. Romanato, "Absorption profile modulation by means of 1D digital plasmonic gratings," Opt. Express **18**(19), 19558–19565 (2010).
17. D. Crouse, and P. Keshavareddy, "Role of optical and surface plasmon modes in enhanced transmission and applications," Opt. Express **13**(20), 7760–7771 (2005).

#141058 - $15.00 USD Received 12 Jan 2011; revised 28 Feb 2011; accepted 16 Mar 2011; published 29 Apr 2011

18. F. Marquier, J. J. Greffet, S. Collin, F. Pardo, and J. L. Pelouard, "Resonant transmission through a metallic film due to coupled modes," Opt. Express **13**(1), 70–76 (2005).
19. L. Rayleigh, "On the dynamical theory of gratings," P. Roy. Soc. Lond. A. Mat. **79**(532), 399–416 (1907).
20. H. Raether, *Surface Plasmons* (Springer-Verlag, Berlin, 1988).

1. Introduction

Since the discovery of the Extraordinary Optical Transmission (EOT) [1–3], plasmonic gratings have become subject of great interest. Despite EOT has been discovered on 2D arrays of holes, 1D metallic gratings have become soon object of study, since this geometry is easier to threat. In particular, 1D geometry represents the ideal choice for the transmission analysis of TE and TM polarization. Theoretical studies, performed using different analytical and computational methods [4–7], showed that the optical response of a metallic grating is given by a combination of three main phenomena [8,16]: Surface Plasmon Polaritons (SPPs) resonances, whose nature can be only TM, cavity mode resonances (CM), and Wood-Rayleigh anomalies that can be excited both for TE and TM polarization.

Since SPPs do exist only for TM-polarization, this case was studied mainly, whereas few references report investigation about TE-polarization transmission properties. Although these resonances have a different field distribution compared to TM case, they lead to transmission efficiency with intensity comparable to the TM case. One of the works that treated the s-polarization case is the one presented by Crouse *et al.* [9] in 2007. In this work it is shown that even for s-polarization (TE), cavity modes resonances in 1D metal-dielectric structures can occur. In particular, by placing inside the grooves a high dielectric constant material, they present a computation focused to optimize EOT for TE and TM polarization simultaneously. The polarization dependence was also investigated by Lu et al. [10] in 2008 for pure metallic gratings in the infrared part of the electromagnetic spectrum and by Marquier et al. [11] in 2008 where the influence of polarization on thermal emission was studied.

Experimental analyses of 1D gratings are much less than those performed on 2D gratings. Barbara et al. [12] in 2002 presented a first study in the optical regime, using a silica grating covered with gold. Later, Pang et al. [13] presented an experimental study in which different geometrical grating's parameters were analysed. In both cases only the p-polarization case was studied deeply. Other two experimental studies on 1D gratings were presented by Crouse et al. [14] in 2008 and Collin et al. [15] in 2010. These studies were performed in the microwave spectral region for p and s-polarization and for p-polarization and in the infrared spectral regime respectively.

The aim of this paper is to show, both experimentally and numerically, that under particular conditions EOT trough 1D gold grating becomes polarization independent in the optical regime. This study provides correlation between the far field and near field analysis of the optical modes involved in the transmission process. The numerical analysis performed as function of period and wavelength allows to describe the limits of the phenomenon.

2. Fabrication and optical characterization

The fabrication process of 1D gold gratings is made by means of an Electron Beam Lithography (EBL) system JEOL 6300FS operating at 100 keV, with 2 nA current, on a glass substrate coated with 350nm of PMMA resist. The typical chip patterned area has a dimension of 2x2 mm^2. After the resist patterning, the metallic structures were obtained by means of electrolytic growth. A thin layer of ITO on the substrate acts as conductive layer necessary for the electric contact during the galvanic growth. A growth current of 100 mA, voltage of 2.9 V and growth time of 45 sec has been used. The growth rate was calibrated to be 3.3 nm/sec. A typical fabricated gold grating is shown in Fig. 1.

#141058 - $15.00 USD Received 12 Jan 2011; revised 28 Feb 2011; accepted 16 Mar 2011; published 29 Apr 2011

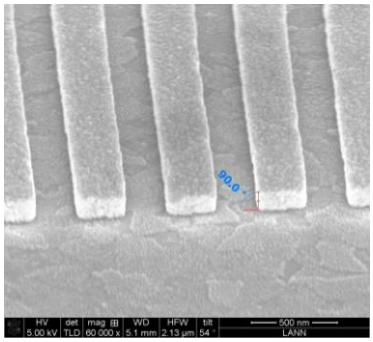

Fig. 1. Example of a fabricated gold grating. It's clearly visible the ITO structure underneath the gold ridges.

The optical characterization of the samples is made through ellipsometric measures; in particular we focus on the far-field transmission properties of the system. Experimental measures have been performed by using a variable angle spectroscopic ellipsometer (J.A.Woollam Co.). The equipment allows to perform measurements over a wide spectral range from 193nm up to 2200nm and its variable wavelength and polarization angle of incidence light allows flexible measurements. In particular, our measurements have been performed at normal incidence, and the polarization angle has been varied from 0° (tangential component of electric field perpendicular to the slits axis - TM) to 90° (tangential component of electric field parallel to slits axis - TE).

3. Numerical simulations

FEM simulations have been performed using COMSOL Multiphysics, RF package. In order to minimize computational time and to improve precision, the full EM fields distributions have been computed with FEM only in one period of the grating, setting periodic boundary conditions. The simulated structure includes both the ITO and glass substrate along with two layers of PML (Perfectly Matched Layer) on the upper and lower sides of the geometry. The ratio between slit width and period (duty cycle) is kept constant to 50%, in order to have resonances for both TE and TM polarization and match the value of the experimental sample. The metal thickness is fixed to a value of 200 nm, and the light impinges normally to the sample. The dielectric constants of the metal and different substrates are taken directly from ellipsometric experimental measures performed on the samples used for the experiment.

4. Results and discussion

In Fig. 2a is reported a transmission spectra for a 1D gold grating (period 516 nm, slit width 258 nm and metal thickness 200 nm) as function of incident wavelength, for different polarization angles. The transmission reaches a remarkable value as high as 55% for the TM polarization.

#141058 - $15.00 USD Received 12 Jan 2011; revised 28 Feb 2011; accepted 16 Mar 2011; published 29 Apr 2011

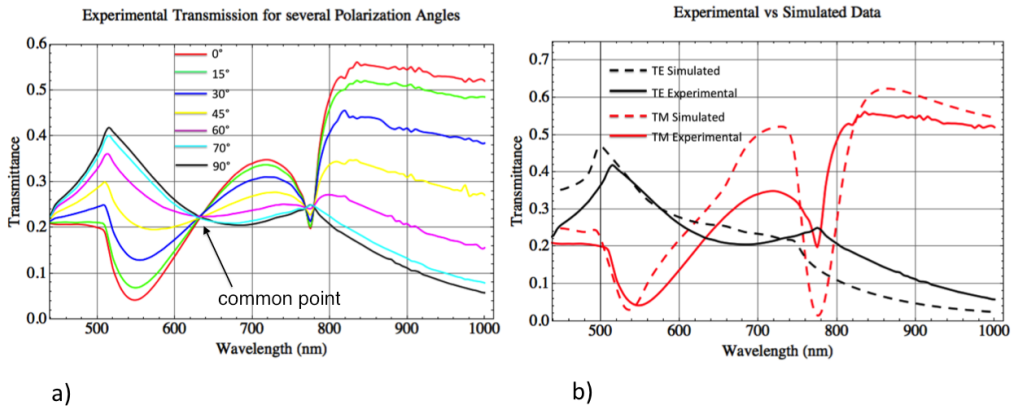

Fig. 2. (colour online) a) Experimental transmission spectra as function of incident light wavelength and polarization angle, from 0° (TM) to 90° (TE). At 630nm a point common to all polarization values is observed. b) Comparison between experimental (continuous lines) and simulated (dashed lines) data for TE and TM transmission spectra.

Different features in the transmission spectra appear for TM and TE polarization. Three kind of mechanism are responsible for the peculiar transmission properties of the system: Surface Plasmons Polaritons (SPP) resonances, Cavity Modes (CM) resonances, and Wood-Rayleigh (WR) anomalies [16,17]. These different types of resonances can couple in different way generating the complex behaviour of the transmitted spectra (Fig. 2a). CM is a single mode Fabry-Perot like-resonance standing inside the slits, which occurs when the phase difference between the different waves transmitted to the substrate is a multiple of 2π. Since this type of resonance can be excited for both TE and TM polarizations, any given combination of the two fundamental polarizations can give rise to a CM. SPP resonances are due to the matching between the in-plane component of the TM polarized incident radiation and the grating vector $G=2\pi/d$ (where d is the grating's period):

$$nG = k_0 \,\mathrm{Re}\left(\sqrt{\frac{\varepsilon_d \varepsilon_m}{\varepsilon_d + \varepsilon_m}}\right) \tag{1}$$

and where ε_m and ε_d are the dielectric constants of the metal and the dielectric (air or substrate depending on the interface considered). SPP resonances are related to transmission extinction and high EM field enhancement at the top surface of the slits [16]. WR anomalies [19] are abrupt changes in transmission that occur both in TE and TM polarization when a diffraction order lies in the plane of the grating, i.e. when:

$$d_n = n\lambda / N \tag{2}$$

where n is the diffraction order, d the period, N the refractive index of the substrate and λ the wavelength. These configurations mark a discontinuity since for $d>d_n$ the n-th diffraction order does exist while for $d<d_n$ it does not. It's worth noting that WR are not resonant phenomena but are due to geometrical parameters and are not related to CM and SPP. Both Eq. (1) and Eq. (2) refer to normal incidence.

In the experimental spectrum (Fig. 2a) we observe all of these features. In Fig. 2b is reported a comparison between an experimental spectrum and a simulated one, for both TE and TM polarization. As we can see, the spectral locations of cavity modes and transmission dips are in fairly good agreement with theoretical data, discrepancies being due to fabrication artefacts.

For TM polarization we see that at a wavelength of 550 nm a transmission dip is present. The dip spectral location is very close to the one predicted by Eq. (1) (at 550 nm the dielectric

#141058 - $15.00 USD Received 12 Jan 2011; revised 28 Feb 2011; accepted 16 Mar 2011; published 29 Apr 2011

constant of the gold is ε_m=–6+2.09i), thus confirming the plasmonic nature of this anti-resonance. In fact, at this wavelength, SPP are excited on the air-gold interface of the grating, and the electromagnetic (EM) field is confined on the top of the metallic structures, leading to transmission extinction and high near-field enhancement [17]. The peak at 720 nm is due to a hybrid SPP-CM mode formed by the combination of planar SPP on the top of the grating and by SPP cavity modes excited on the vertical walls of the slits [17]. In fact, as many authors pointed out, CMs and SPPs resonances are not independent each other [18] and they can couple in order to generate a hybrid mode that presents both CM and SPP resonant characteristics. The transmission dip at 775 nm is another SPP excitation; this time SPP are excited on the gold-ITO interface of the grating (at 775 nm the dielectric constants of the gold and ITO substrate are respectively ε_m=–24+1.62i and ε_d=2.28+0.077i). Finally at a wavelength of 850 nm a more intense CM mode is excited, reaching a sort of plateau in the transmission spectrum. For this type of resonance, the EM field is distributed uniformly within the slits [17].

For TE polarization, SPPs cannot be excited [20]; although the resonance observed for this polarization at a wavelength of 516 nm (equal to grating's period) is due to the excitation of a cavity mode, the EM field distribution within the slits is completely different respect to the TM case. For this polarization, the field is located at the centre of the slits, with no SPP field mode located on the vertical walls. These cavity modes strongly depends on the geometry of the slits and grating, like slits width and metal thickness [9,10]. For TE polarization we also observe a WR anomaly, represented by a less intense transmission peak located at 780 nm. Its spectral location is well predicted by Eq. (2) (the refractive index of the ITO substrate at 780 nm is N=1.517+0.025i), thus confirming the nature of this peak.

Experimental data also clearly show that, by a rotation of polarization from 0° to 90°, all the spectral features have a progressive suppression or enhancement and that the TM spectrum gradually transform into the TE one. A peculiar behaviour is represented by a "*common point*" for all the different polarization angles, located at a wavelength of about 630 nm and having a transmission of 23%. This point represents a symmetry of the system: at that particular wavelength, no matter the polarization angle, the far field transmission remains constant.

The polarization independence, however, does not hold also at microscopic level where the EM configuration changes dramatically. Switching from TE to TM polarization, the resonant EM field distribution inside the slits changes from a cavity mode to a direct SPP excitation, as shown by the FEM simulations at common point wavelength, reported in Fig. 3

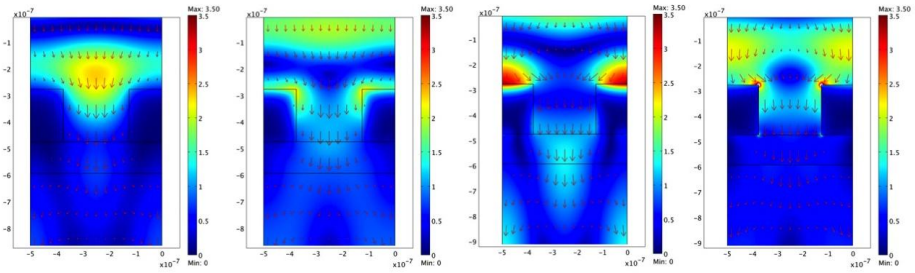

Fig. 3. (colour online) FEM simulation of EM field configuration and average power flow at the common point wavelength (630nm) for a gold grating with period of 516 nm, duty cycle set to 50% and gold thickness of 200nm. The colour scale is normalized to the incident EM field a) and b) TE polarization, electric and magnetic field respectively c) and d) TM polarization, electric and magnetic field respectively.

#141058 - $15.00 USD Received 12 Jan 2011; revised 28 Feb 2011; accepted 16 Mar 2011; published 29 Apr 2011

For TE polarization (Fig. 3a) the norm of electric field has its maximum localized in the centre of the slits, while the magnetic field is located mostly in the upper region of the grating (Fig. 3b). For TM polarization (Fig. 3c,d) the norm of the EM fields presents both the typical SPP excitation on the upper side of the grating, related to transmission extinction, and a cavity mode field pattern within the slits, which leads to EOT [14]. Thus, contrary to the far field behaviour, at *common point* the EM field keeps strong polarization dependence. Thanks to Maxwell's equations linearity, however, the two completely different near-field behaviours combine linearly and give rise to the polarization-independent transmittance spectra experimentally observed (Fig. 2a). This is confirmed by the average power outflow (red arrows in Fig. 3), which is very similar for both polarizations. Is the *common point* found for this sample a real singularity? In order to answer this question we have performed multiparametric FEM simulations that allow to explore the phase map and look for the configurations which show to be polarization independent. In Fig. 4a and Fig. 4b the transmission maps are reported as function of incident wavelength and grating period respectively for TM and TE polarization.

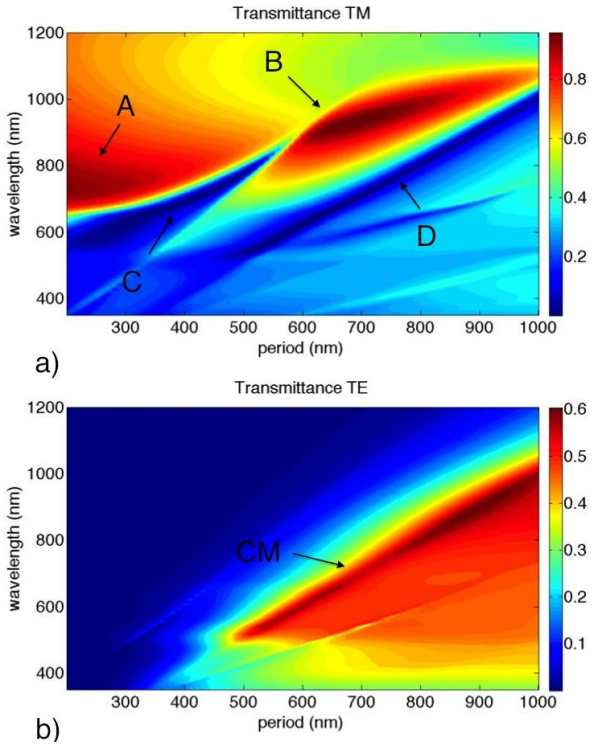

Fig. 4. (colour online) FEM transmission map (colour scale) as function of grating's period and incident light wavelength. The duty cycle is kept fixed to 50% and the gold thickness is set to 200nm. Fig. a) refers to TM case. Fig. b) refers to TE case. The letters refers to the different transmission resonances described in the main text.

For TM two distinct high-transmission areas are present, corresponding to both hybrid cavity modes-SPP and CM resonances. The first one (marked with A on the map) is located in the low-period region of the map, and starts at a wavelength of 670 nm up to 1000 nm. The second one (marked with B) is located at higher period values (stating from 600 nm) but has a narrower wavelength bandwidth compared to the previous one. In this map are also presents anti-transmission bands; the first one (marked with C) corresponds to period values in the range from 250 to 550 nm, while the second one (marked with D) is located at period values higher than 550 nm. These bands correspond to direct SPP excitation at the different

#141058 - $15.00 USD Received 12 Jan 2011; revised 28 Feb 2011; accepted 16 Mar 2011; published 29 Apr 2011

interfaces (air-gold and gold-ITO), as confirmed by their spectral positions, which in first approximation fits the prediction of grating-coupling formula for SPP excitation (Eq. (1). For TE we can see that only cavity modes (marked with CM on the map) are present, as expected. The fact that TE cavity modes appear to wavelengths near the grating period must not be confused with the presence of WR anomalies, as Eq. (2) might suggest, but instead to the particular geometry we have choose in our analysis. In fact TE cavity modes are strongly dependent on slits width [9,10] and metal thickness and in our calculations we found that if these two parameters are varied, the TE cavity modes are strongly modified (both spectral location and transmission intensity).

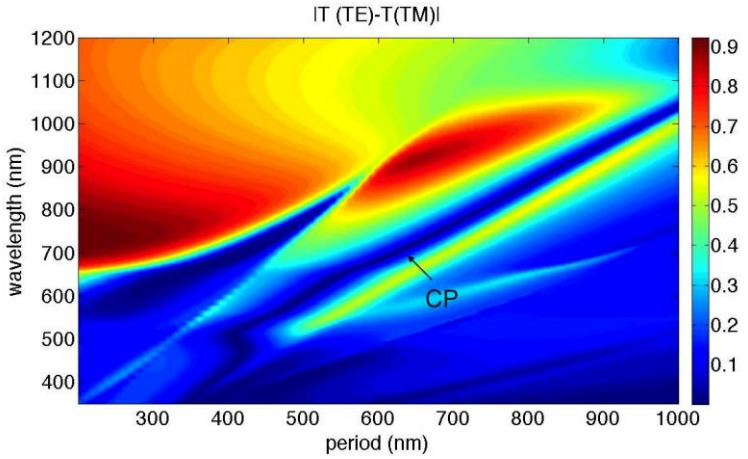

Fig. 5. (colour online) FEM map that plots the absolute difference between TE and TM transmission values (Fig. 4) as function of incident light wavelength and grating's period. Letter CP refers to the "common point" band.

In order to study the properties of the common point, we made also a map that plots the absolute value of the difference between TE and TM transmission (Fig. 5). Since at the *common point* the transmission is the same for both polarizations, we expect to see in the map transmission minima corresponding to the common point. In fact, a *common point* band appears (marked with CP), starting from a wavelength of 500 nm and up to 1050 nm. This band represents the dependence of the common point on grating's period and wavelength. As we can see, the spectral location of common point as function of period follows an almost linear dependence behaviour; this means that we can choose the particular wavelength at which the common point occurs just by varying the grating's period. This can be useful exploited to design the common point configuration at a particular wavelength. It's worth noting that for this kind of structures the absorption has significant value (values between 40% and 80%) only in the low-wavelength regime of the spectrum (from 350 to 500 nm). For longer wavelengths, the absorption drops significantly up to less than 3%. This means that the transmittance and reflectance for wavelengths larger than 500 nm are complementary each other, thus opening the possibility to obtain also a reflectance polarization independence.

5. Conclusions

Transmission trough 1D gold grating has been studied both experimentally and numerically. Transmission spectra show EOT for both TE and TM polarization, although with different transmission mechanisms, reaching a maximum transmission value of 55% for the TM case. The polarization dependence of the system shows a symmetry property highlighted by the presence of a point common to all the different polarization angles. FEM simulations were used in the analysis in order to understand the transmission properties of the system both on

#141058 - $15.00 USD Received 12 Jan 2011; revised 28 Feb 2011; accepted 16 Mar 2011; published 29 Apr 2011

the near and far field regime. In particular we have shown that the far-field polarization independence does not hold on the near-field regime. These preliminary results can be usefully exploited for bio-sensoristic applications, when a highly sensitive response to functionalization is needed. 2D maps allow to point out the different aspects involved in the transmission process for the two fundamental TE and TM polarizations, showing the presence of a common point band whose spectral location depends linearly on grating's period.

Acknowledgments

This work has been supported by a grant from "Fondazione Cariparo" - Surface PLasmonics for Enhanced Nano-Detectors and Innovative Devices (SPLENDID) and from ORION project of European Community, grant agreement n. 222517.

#141058 - $15.00 USD Received 12 Jan 2011; revised 28 Feb 2011; accepted 16 Mar 2011; published 29 Apr 2011